Journal of Hazardous Materials 181 (2010) 586–592

Contents lists available at ScienceDirect

Journal of Hazardous Materials

journal homepage: www.elsevier.com/locate/jhazmat

Templated preparation of porous magnetic microspheres and their application in removal of cationic dyes from wastewater

Qingquan Liu[a,b], Li Wang[a,*], Anguo Xiao[a], Jingming Gao[a], Wenbing Ding[a], Haojie Yu[a], Jia Huo[a], Mårten Ericson[a,c]

[a] State Key Laboratory of Chemical Engineering, Department of Chemical and Biological Engineering, Zhejiang University, Zheda Road 38, Hangzhou 310027, China
[b] College of Chemistry and Chemical Engineering, Hunan University of Science and Technology, Xiangtan 411201, China
[c] Department of Industrial Ecology, Royal Institute of Technology, SE-100 44 Stockholm, Sweden

ARTICLE INFO

Article history:
Received 19 January 2010
Received in revised form 5 May 2010
Accepted 13 May 2010
Available online 21 May 2010

Keywords:
Magnetic microspheres
Cationic dye
Removal
Regeneration

ABSTRACT

Porous magnetic microspheres with large particle size (350–450 μm) were prepared with sulfonated macroporous polydivinylbenzene as a template. The preparation process included ferrous ion exchange and following oxidation by hydrogen peroxide. The results showed that the weight fraction of magnetic nanoparticles exceeded 20 wt% in microspheres after the preparation process was repeated three times. X-ray diffraction profiles indicated that the crystalline phase of as-formed magnetic nanoparticles was magnetite (Fe_3O_4). TEM images revealed rod-like magnetite crystal after the first oxidation cycle, however, the crystal morphologies were transferred into random shape after more oxidation cycles. The applicability of porous magnetic microspheres for removal of cationic dyes from water was also explored. The results exhibited that basic fuchsin and methyl violet could be quickly removed from water with high efficiency. More importantly, the magnetic microspheres could be easily regenerated and repeatedly employed for wastewater treatment. Therefore, a novel methodology was provided for fast removal cationic dyes from wastewater.

1. Introduction

Magnetic nanoparticles (MNPs) are currently being intensively investigated because of their extensive applications such as drug release [1–4], magnetic resonance imaging [5–8], biological separation [9,10] and water purification [11,12]. Among them, water purification with magnetic materials is a new research subject, which was reported by only a few papers. For example, the work by Yavuz et al. reported successful removal of arsenic from wastewater using monodisperse superparamagnetic nanoparticles [11]. But it is difficult to reuse superparamagnetic nanoparticles because the interaction between iron oxides and arsenic is strong and irreversible. Zhao et al. [12] employed superparamagnetic microspheres with Fe_3O_4@SiO_2 core and porous SiO_2 shell as a reusable absorbent to remove microcystins from eutrophic water, however, silica is susceptible to be corroded in harsh environment such as strong base media.

Cationic dyes have wide industrial applications such as dyeing of silk, leather, paper, wool and cotton [13]. However, these organic dyes in discharged wastewater often compose a great threat for health of human being and environmental pollution. Therefore, up to now, various techniques like chemical oxidation [14], biological treatment [15], coagulation [16,17], and adsorption [18–24] were explored for removal of cationic dyes. Among them, physical adsorption is generally recognized as a simple and efficient technique. In this regard, ion exchange membranes [18], activated carbon [19], clay [20,21], zeolite [22], and other natural materials [23,24] have been employed for lowering concentration of cationic dyes in wastewater. But it is still difficult to purify wastewater due to some problems in adsorption of cationic dyes by adsorbents, such as high cost for regeneration [18], low flow rate [19], and difficult separation of absorbent from wastewater [23]. Hence, attempts to explore novel adsorption materials and treatment process for removal of cationic dyes from wastewater will be valuable.

Recently, magnetically driven separation has shown a very positive impact in liquid-phase catalytic field because it makes the recovery of catalysts from liquid phase quite easy and simple [24–26]. We think magnetically driven separations could be also utilized in the field of wastewater treatment for fast separation of absorbents from water. This process may be helpful to solve the problem about difficult recovery of absorbent. Furthermore, considering that wastewater may be

* Corresponding author. Tel.: +86 571 87953200; fax: +86 571 87951612.
E-mail address: opl_wl@dial.zju.edu.cn (L. Wang).

0304-3894/$ – see front matter © 2010 Elsevier B.V. All rights reserved.
doi:10.1016/j.jhazmat.2010.05.053

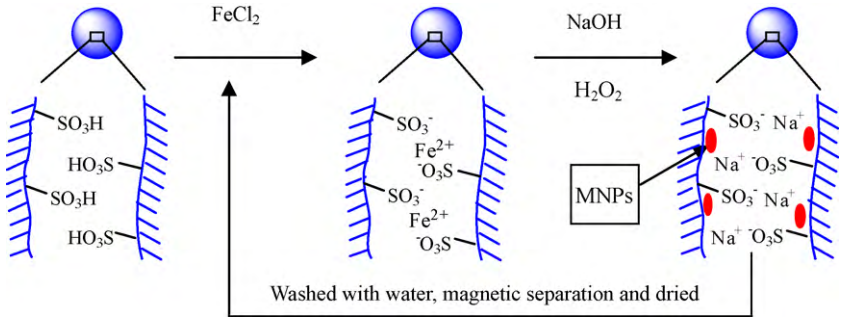

Fig. 1. Schematic illustration of preparation of porous magnetic microspheres. : magnetic nanoparticles (MNPs).

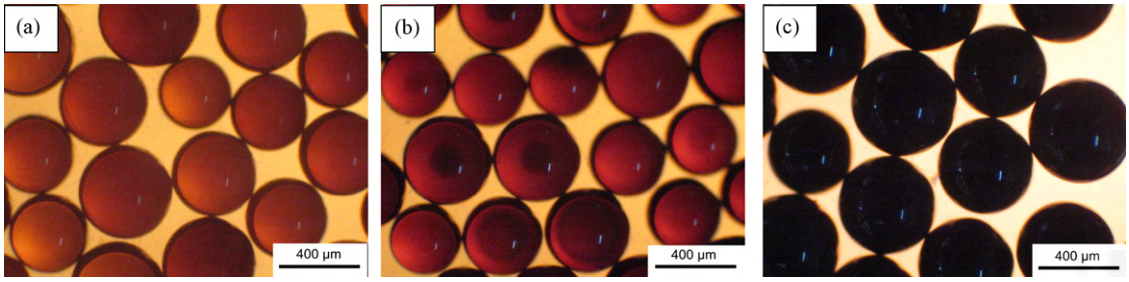

Fig. 2. Optical microscope images of PDVB–SO_3H (A), PDVB–Mag1 (B), and PDVB–Mag4 (C).

acidic or alkaline, magnetic adsorbents based on polymer materials may be more suitable for wastewater treatment. With this in mind, the objective of the present study is to prepare porous magnetic microspheres (PMMs) with macroporous polydivinylbenzene (PDVB) microspheres as a template, and to repeatedly use for removal of cationic dyes from wastewater. To the best of our knowledge, this is the first time to use PMMs for removal of cationic dyes. Macroporous PDVB microspheres were prepared with toluene as an inert porogen in our lab [27–29]. For convenient recycling PMMs, macroporous microspheres with large particle size and narrow size distribution (350–450 μm) were employed for fabrication of PMMs in the present study.

2. Experimental

2.1. Sulfonation of macroporous PDVB microspheres

Macroporous PDVB microspheres (3.02 g) with diameter of 350–450 μm and dichloromethane (75.0 mL) were added into a 250 mL three-neck bottle. The solution was cooled to 0 °C in an ice bath, before another 75.0 dichloromethane containing 0.8 mL chlorosulfuric acid was dropwise added into the stirred solution. Then, the reaction was performed at room temperature for 24 h with magnetic stirring. The sulfonated products were filtrated by a sintered glass funnel, and washed by dichloromethane for three times. After dried in a vacuum oven, the sulfonated microspheres were washed with deionized water for five times, and dried in vacuum oven. The sulfonated microspheres were marked as PDVB–SO_3H.

2.2. Preparation of porous magnetic microspheres

PMMs were prepared according to the routes proposed by Ziolo et al. [25] with some modifications. Sulfonated PDVB microspheres (2.10 g) and $FeCl_2$ solution (80.0 mL, 1.0 mol/L) were added into a 250 mL three-neck bottle with condenser, mechanical stirrer and argon inlet. The solution was stirred in room temperature for 24 h to perform enough ion exchange. The products were separated by sintered glass funnel, and were washed with deionized water for several times until no Fe^{2+} was detected in the eluent by sodium thiocyanide. After the products were transferred into

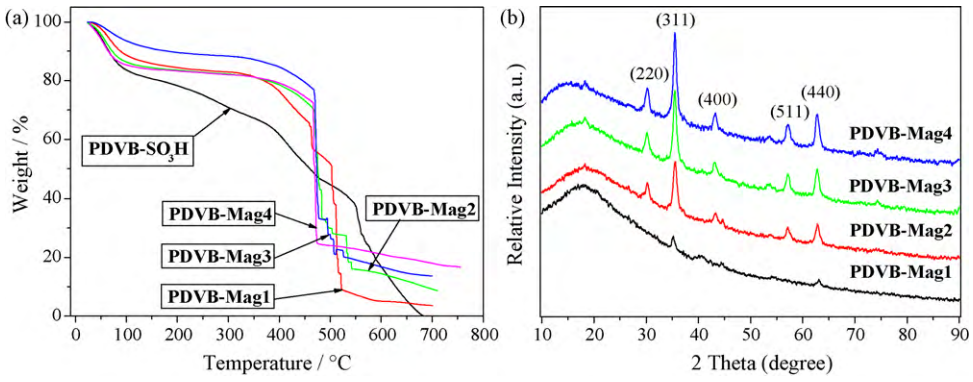

Fig. 3. TGA curves (A) and X-ray diffraction patterns (B) of PDVB–Mag1, PDVB–Mag2, PDVB–Mag3, and PDVB–Mag4.

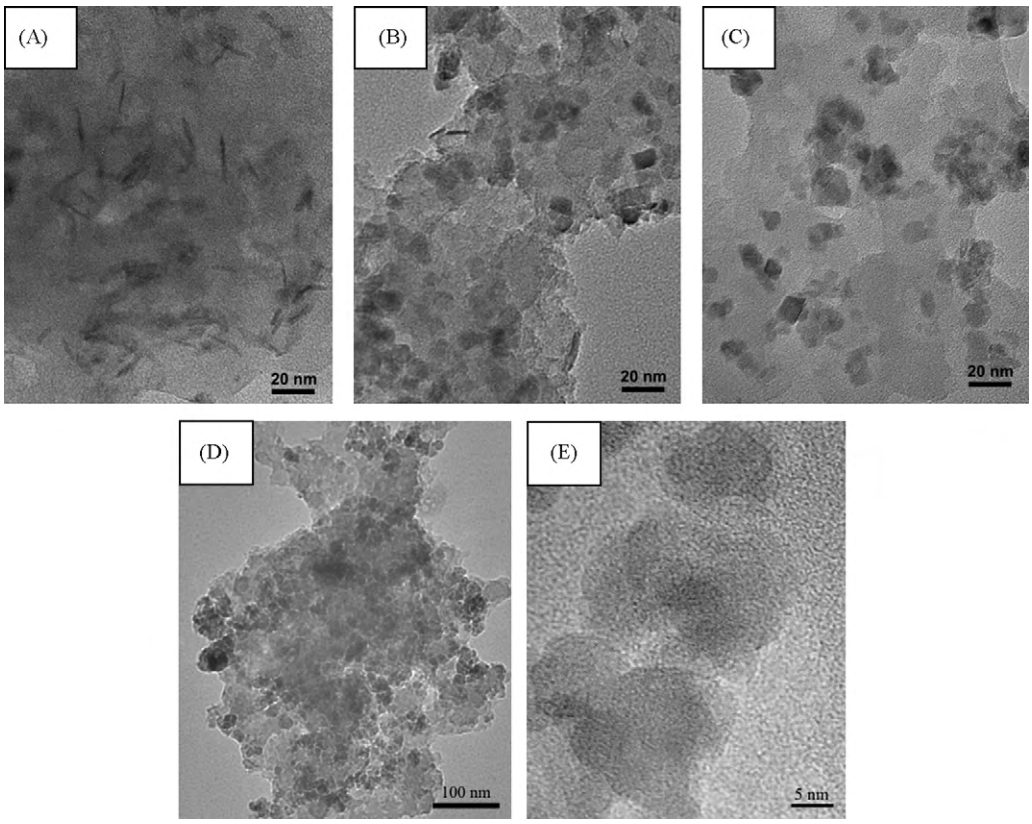

Fig. 4. TEM images of PDVB–Mag1 (A), PDVB–Mag2 (B), PDVB–Mag3 (C) and PDVB–Mag4 (D and E).

another three-neck reactor, 50.0 mL deionized water and 50.0 mL NaOH solution (3.5 mol/L) were added. Then, the mixture was heated and stirred at a speed of 200 rpm. After the temperature of oil bath reached 75 °C, hydrogen peroxide solution (20.0 mL, 30 vol%) was dropwise added into the mixture. The solution was kept at 75 °C for 2 h. The final products were washed with deionized water until the eluent was neutral. Finally, the brown products were dried in a vacuum oven at 60 °C. In order to improve the weight fraction of iron oxide, the above process was repeated three times.

2.3. Characterization

Sulfonation degree of PDVB was determined by acid–base titration. Firstly, PDVB–SO_3H microspheres were ground as fine as possible in a mortar. Then, a certain amount of ground PDVB–SO_3H powders were suspended in deionized water. The suspended solution was titrated by NaOH standard solution in the presence of phenolphthalein as an indicator. Note that when the titration was approaching the endpoint, the suspension solution was dispersed by ultrasonic for 1 min to ensure reaching the balance of acid–base reaction. If suspension solution still keeps red, we think the titration endpoint has reached.

Nitrogen sorption porosimetry was performed on a micromeritics ASIC-2. The experiments were carried out at the temperature of liquid nitrogen (77.3 K). The samples were first heated in a tube under vacuum at 70 °C for 12 h to remove adsorbed materials from the surface. The data were manipulated using the software supplied to yield the relevant porosity parameters.

Thermogravimetric analysis (TGA) of sulfonated and magnetic microspheres was performed on a Perkin-Elmer TGA-7. In a flow of air, the heating rate is 10 °C/min from 20 °C to 700 °C.

X-ray diffraction pattern of PDVB–Mag was determined on a D/max-rA XRD instrument using a copper X-ray source.

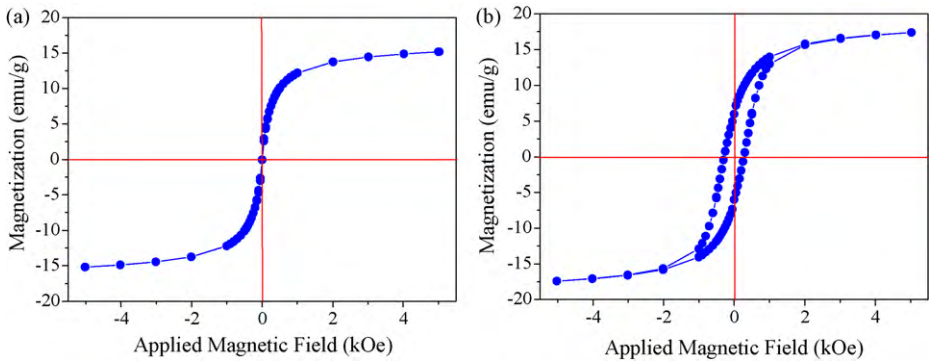

Fig. 5. Magnetization curves of PDVB–Mag4 at 300 K (A) and 5 K (B).

Transmission electron microscopy (TEM) micrographs were obtained on a JEOL model 1200EX instrument operated at an accelerating voltage at 160 kV. For TEM analysis, PMMs were also ground as fine as possible, and the powder was dispersed in ethanol.

Optical microscopy photos were taken on a NOVEL XS-2100 microscope instrument.

A SQIUID magnetometer was used for measurement of magnetization curves in the fields up to 4000 kA/m at room temperature.

2.4. Removal of basic fuchsin and methyl violet by PMMs

Basic fuchsin (BF) solution (3.25 mL, 2.802×10^{-5} mol/L) and 0.2 g PMMs were added into a glass bottle, which was dispersed by ultrasonic for 5 min. After separated by a magnet, the solution was collected and marked as BF-1. Then, 3.25 mL anhydrous ethanol was added into the bottle containing PMMs, which was sonicated for 5 min to regenerate PMMs. After magnetic separation and removed the extracted solution, another 3.25 mL BF solution was again added into the bottle and repeated the above process. The collected BF solution was labeled as BF-2, BF-3, and BF-4, respectively. Removal process of methyl violet (MV, 1.328×10^{-5} mol/L) was just the same as that of BF. Concentration of the collected BF and MV solution was determined by a UV751GW ultraviolet spectrophotometer.

3. Results and discussion

3.1. Preparation of PMMs

PDVB and its sulfonated products (PDVB–SO_3H) were characterized by infrared spectra (Fig. S1). Peaks at 1176 cm^{-1} correspond to stretching vibration of S=O in SO_3H [30], which demonstrates successful sulfonation of PDVB microspheres. The sulfonated microspheres were ground as fine as possible, before the sulfonation degree was determined by titration of standard NaOH solution. The results showed the concentration of [SO_3H] was 2.46×10^{-3} mol/g, or the content of sulfur in PDVB–SO_3H was 7.87 wt%. These values are very close to that reported by Winnik et al. [31].

Sulfonated microspheres were firstly exchanged with ferrous ion (Fe^{2+}) at room temperature, and followed by oxidation with hydrogen peroxide under base conditions. As a result, MNPs were formed and interspersed on the pore wall. Fig. 1 presents the schematic illustration of the preparation of PMMs. In order to improve the fraction weight of MNPs, the above process was repeated three times again, and resultant products were labeled as PDVB–Mag1, PDVB–Mag2, PDVB–Mag3, and PDVB–Mag4, respectively. It is worth noting that the specific surface area of PDVB microspheres derived from N_2 sorption was 701 m^2/g, however, that value of PDVB–Mag4 was reduced to 239 m^2/g. This fact demonstrated that MNPs were successfully deposited into the pores of macroporous templates through oxidation of ferrous ion.

The optical microscope images of PDVB–SO_3H, PDVB–Mag1, and PDVB–Mag4 are shown in Fig. 2. Obviously, PDVB–SO_3H microspheres are of optical transparency to some extent. However, optical transparency declined progressively after MNPs were incorporated into the microspheres, and PDVB–Mag4 became completely opaque. In addition, with increasing the repeated times, the average particle size of PMMs slightly increased because microsphere's surface was coated by some MNPs.

3.2. Characterization of PMMs

Thermogravimetric analysis (TGA) curves of PMMs are shown in Fig. 3A. PDVB–SO_3H could be entirely burned out under an air atmosphere at the temperature of 681 °C. The major decomposition region of PMMs was 450–500 °C, and the weight fraction of MNPs in PDVB–Mag1 was about 8.8 wt%. The value was improved with increasing the repeated times. After repeated three times (PDVB–Mag4), the weight fraction of MNPs exceeded 20 wt%. We believe that the value could be furthermore improved by more repeated times. Therefore, controllable preparation of PMMs with different weight fraction of MNPs can be achieved by this synthetic route.

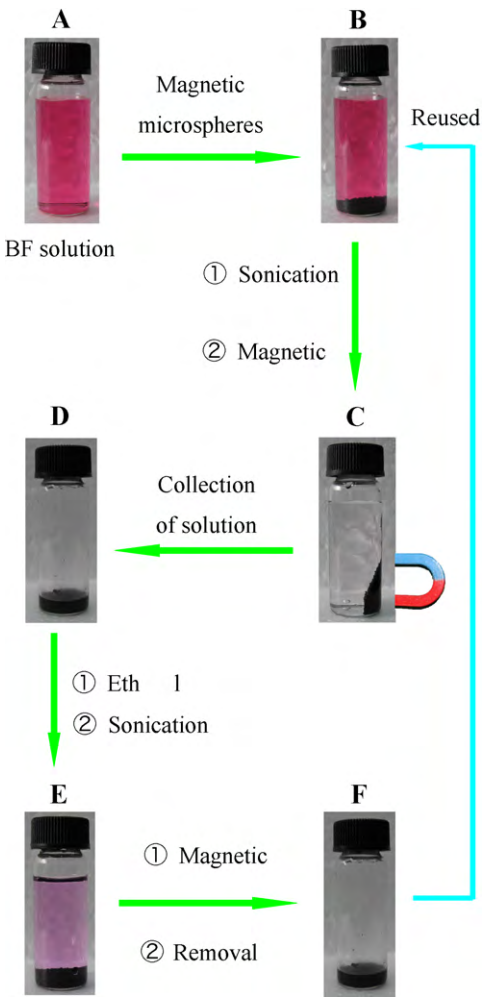

Fig. 6. Schematic illustration of magnetic separation of basic fuchsin (BF) from aqueous solution, and regeneration of PMMs.

X-ray diffraction was employed for determining crystalline phase of MNPs. Fig. 3B indicates that the crystalline phase of MNPs was Fe_3O_4, because five diffraction peaks at $2\theta = 30.1°$, 35.5°, 43.2°, 57.4°, 62.9° were the characteristic peaks of standard magnetite (Fe_3O_4) crystal [32]. Furthermore, XRD profiles of all samples were identical, indicating that the MNPs structure remained essentially unchanged during oxidation of ferrous ions. Obviously, the relative diffraction intensity of the magnetite peaks became stronger from PDVB–Mag1 to PDVB–Mag4. We think higher MNPs fraction could be responsible for that.

Transmission electron microscope (TEM) images showed that MNPs in PDVB–Mag1 (Fig. 4A) were rod-like. Maybe there are two factors responsible for that shape. First, the macropores in PDVB–SO_3H provide enough space for Fe_3O_4 crystal growth during the first oxidation, therefore, the crystal grows along a preferred direction, namely, orientation of pore channel. Second, thermodynamic theory indicates that heterogeneous nucleation needs lower

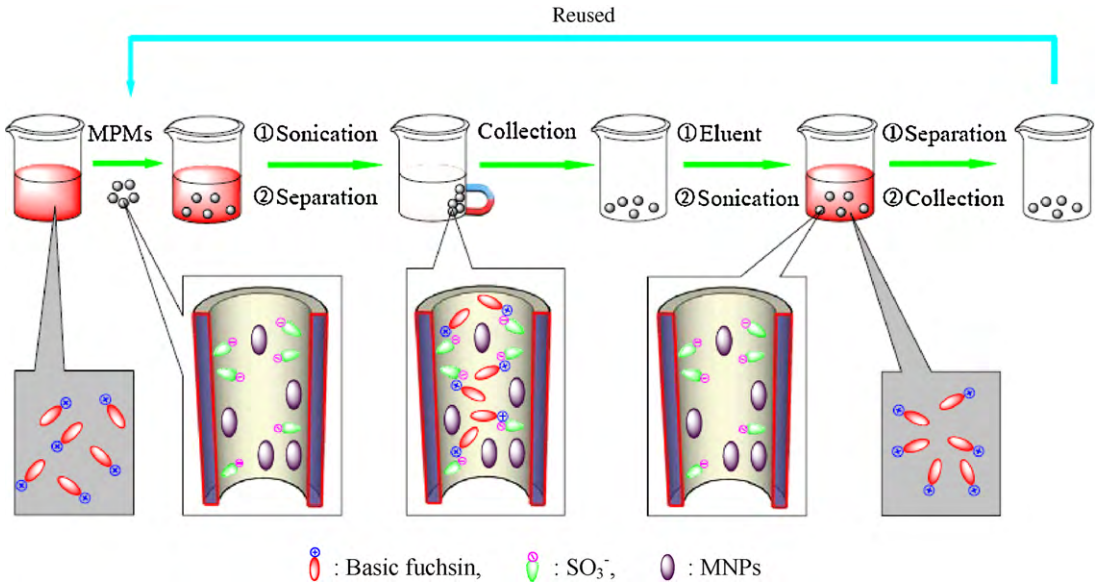

Fig. 7. Mechanism of adsorption BF by PMMs and desorption of BF by anhydrous ethanol. : basic fuchsin, : SO_3^-, : MNPs.

activation energy than homogeneous nucleation. Consequently, Fe_3O_4 crystal may be nucleated by the pore wall and grown along the direction in parallel with pore wall. Furthermore, this opinion was indirectly supported by the size of rod-like crystals, which was 3–7 nm in diameter and 15–30 nm in length. Pore size distribution curves derived from N_2 sorption indicated that there were seldom pores bigger than 30 nm (Fig. S2). Therefore, if Fe_3O_4 crystal grew along the direction perpendicular to the pore wall, the probability to get crystals with diameter of 30 nm was very low.

After the second crystal growth, morphologies of the main MNPs (Fig. 4B) were converted into random shape, which is easy to understand. The second crystal growth was performed on the basis of the rod-like crystals. In comparison with the "rod" end, the "rod" side had a faster crystal growth speed due to higher surface area, which resulted in random shape crystals. No rod-like crystals can be observed after the third (Fig. 4C) and the fourth crystal growth (Fig. 4D). High magnification image (Fig. 4E) revealed that MNPs were about 20 nm in diameter, and had a good crystal structure. However, the main crystals obtained by Winnik et al. [31] were need-like after the fifth crystal growth. We think different pore structure of templates may be responsible for different crystal shapes.

Magnetization curves of PDVB–Mag4 at 300 K and 5 K are presented in Fig. 5. The plots at room temperature (Fig. 5A) showed no hysteresis loop, indicating superparamagnetic property for PMMs. In contrast, curves at 5 K (Fig. 5B) revealed obvious ferromagnetism with a saturation magnetization of 15.2 emu/g, coercivity of 277 Oe and remanence of 6.14 emu/g.

3.3. Removal of cationic dyes by PMMs

Basic fuchsin (BF) and methyl violet (MV) (Fig. S3) are widely used as coloring agents for textile and leather materials. For removal BF or MV from wastewater, several types of materials were employed as adsorbents such as cationic exchange membranes [18], fly ash [33–35], fungal biomass [36], hydrogel [37,38], and perlite [38]. However, problems of difficult separation of adsorbents from wastewater or low accessible flow rate remain to be further solved. Here, we attempt to explore the applicability of PMMs for removal of BF and MV from wastewater. High porosity and large numbers of sulfonic groups interspersed on the pore wall were beneficial to adsorb BF or MV molecules, while magnetic property makes convenience to quickly separate adsorbents from wastewater via an external magnetic field. In order to reuse the magnetic adsorbents, anhydrous ethanol was employed for extracting BF or MV from the adsorbents. The schematic illustration of dye removal and adsorbent regeneration is presented in Fig. 6.

PDVB–Mag4 (0.2 g) was used for removing BF (2.802×10^{-5} mol/L) or MV (1.328×10^{-5} mol/L) from aqueous solution and separated with an external magnetic field. Obviously, the solution of BF or MV turned into colorless or light color after magnetic separation (Fig. 6C), indicating successful adsorption and separation. According to the molecular structures

Table 1
Removal efficiency of BF and MV by PMMs for four cycles.[a].

Cycle	BF-1	BF-2	BF-3	BF-4
Residual BF conc. ($\times 10^{-5}$ mol/L)[b]	0.026	0.069	0.079	0.228
BF removal efficiency (%)	99.1	97.5	97.2	91.8
	MV-1	MV-2	MV-3	MV-4
Residual MV conc. ($\times 10^{-5}$ mol/L)[b]	0.096	0.137	0.170	0.182
MV removal efficiency (%)	92.7	89.7	87.2	86.3

[a] Concentration of original BF and MV solution is 2.802×10^{-5} mol/L and 1.328×10^{-5} mol/L, respectively.
[b] Residual BF or MV concentration after adsorption and magnetic separation.

(Fig. S3), there is one positively charged group (tertiary ammonium group) for molecule of BF or MV. Therefore, electrostatic interaction between tertiary ammonium groups and sulfonic groups may be responsible for adsorption of BF by PMMs, as shown in Fig. 7.

After extracted with anhydrous ethanol, the solution recovered the original color (Fig. 6E), indicating that BF was successfully extracted from PMMs. The possible explanation is that the electrostatic interaction between tertiary ammonium group and sulfonic group could be disrupted by organic solvents such as ethanol [18], as shown in Fig. 7. The process of adsorption, separation and extraction were repeated three times. After adsorption and magnetic separation, the collected solution was labeled as BF-1, BF-2, BF-3, and BF-4, respectively. The concentration of the collected BF and MV solution was calculated from the standard curves (Fig. S4), which were obtained by standard BF or MV solution and their UV absorbency. The data are given in Table 1.

The results indicated that 99.1% BF, and 92.7% MV could be quickly removed after the first cycle (BF-1 and MV-1). We think such high removal efficiency should be attributed to numerous accessible mesopores and sulfonic groups on the pore wall. With increasing cycles, the concentration of collected BF (BF-2–BF-4) and MV (MV-2–MV-4) was slightly increased. After the fourth cycle, more than 90% of BF, and 85% of MV could be effectively removed from aqueous solution, confirming the reusability and high separation efficiency of PMMs. We think slow adsorption kinetics and incomplete desorption of cationic dyes in the last cycle could be responsible for the declined removal efficiency after every cycle.

4. Conclusion

In summary, we have demonstrated the preparation of PMMs with macroporous PDVB as a template. After the 4th crystal growth, the weight fraction of MNPs has exceeded 20 wt%. Furthermore, the shape of MNPs was rod-like after the 1st crystal growth, however, morphologies of MNPs were converted into random shape with increasing the repeated times. The magnetization curves revealed superparamagnetic property for PMMs at room temperature, but ferromagnetism with a saturation magnetization of 15.2 emu/g at 5 K. Finally, PMMs as-synthesized were successfully employed as a reusable absorbent for fast, and convenient removal of cationic dyes from wastewater with high efficiency. Overall, we believe that the approach presented herein provide a convenient way to bind other cationic organic compound or heavy metal ions to magnetic absorbent and to quickly separate them from wastewater.

Appendix A. Supplementary data

Supplementary data associated with this article can be found, in the online version, at doi:10.1016/j.jhazmat.2010.05.053.

References

[1] S.H. Hu, D.M. Liu, W.L. Tung, C.F. Liao, S.Y. Chen, Surfactant-free, self-assembled PVA-iron oxide/silica core–shell nanocarriers for highly sensitive, magnetically controlled drug release and ultrahigh cancer cell uptake efficiency, Adv. Funct. Mater. 18 (2008) 2946–2955.

[2] J.Y. Kim, J.E. Lee, S.H. Lee, J.H. Yu, J.H. Lee, T.G. Park, T. Hyeon, Designed fabrication of a multifunctional polymer nanomedical platform for simultaneous cancer-targeted imaging and magnetically guided drug delivery, Adv. Mater. 20 (2008) 478–483.

[3] N. Nasongkla, E. Bey, J. Ren, H. Ai, C. Khemtong, J.S. Guthi, S.-F. Chin, A.D. Sherry, D.A. Boothman, J. Gao, Multifunctional polymeric micelles as cancer-targeted, MRI-ultrasensitive drug delivery systems, Nano Lett. 6 (2006) 2427–2430.

[4] S.H. Hu, S.Y. Chem, D.M. Liu, C.S. Hsiao, Core/single-crystal-shell nanospheres for controlled drug release via a magnetically triggered rupturing mechanism, Adv. Mater. 20 (2008) 2690–2695.

[5] Y.W. Jun, Y.H. Lee, J. Cheon, Angew, Chemical design of nanoparticle probes for high-performance magnetic resonance imaging, Chem. Int. Ed. 47 (2008) 5122–5135.

[6] J.H. Park, G.V. Maltzahn, L.L. Zhang, M.P. Schwartz, E. Ruoslahti, S.N. Bhatia, M.J. Sailor, Magnetic iron oxide nanoworms for tumor targeting and imaging, Adv. Mater. 20 (2008) 1630–1635.

[7] X.Y. Shi, S.H. Wang, S.D. Swanson, S. Ge, Z.Y. Cao, M.E.V. Antwerp, K.J. Landmark, J.R. Baker, Dendrimer-functionalized shell-crosslinked iron oxide nanoparticles for in-vivo magnetic resonance imaging of tumors, Adv. Mater. 20 (2008) 1671–1678.

[8] H. Lee, E. Lee, D.K. Kim, N.K. Jang, Y.Y. Jeong, S. Jon, Antibiofouling polymer-coated superparamagnetic iron oxide nanoparticles as potential magnetic resonance contrast agents for in vivo cancer imaging, J. Am. Chem. Soc. 128 (2006) 7383–17383.

[9] S.J. Son, J. Reichel, B. He, M. Schuchman, S.B. Lee, Magnetic nanotubes for magnetic-field-assisted bioseparation, biointeraction, and drug delivery, J. Am. Chem. Soc. 127 (2005) 7316–7317.

[10] A.H. Lu, E.L. Salabas, F. Schuth, Magnetic nanoparticles: synthesis, protection, functionalization, and application, Angew. Chem. Int. Ed. 46 (2007) 1222–1244.

[11] C.T. Yavuz, J.T. Mayo, W.W. Yu, A. Prakash, J.C. Falkner, S. Yean, L. Cong, H.J. Shipley, A. Kan, M. Tomson, D. Neatelson, V. Colvin, Low-field magnetic separation of monodisperse Fe_3O_4 nanocrystals, Science 314 (2006) 964–967.

[12] Y.H. Deng, D.W. Qi, C.H. Deng, X.M. Zhang, D.Y. Zhao, Superparamagnetic high-magnetization microspheres with an Fe_3O_4@SiO_2 core and perpendicularly aligned meso-porous SiO_2 shell for removal of microcystins, J. Am. Chem. Soc. 130 (2008) 28–29.

[13] H.M. Eckenrode, S.H. Jen, J. Han, A.G. Yeh, H.L. Dai, Adsorption of a cationic dye molecule on polystyrene microspheres in colloids: effect of surface charge and composition probed by second harmonic generation, J. Phys. Chem. B 109 (2005) 4646–4653.

[14] T. Olmez, I. Kabdasli, O. Tunay, The effect of the textile industry dye bath additive EDTMPA on colour removal characteristics by ozone oxidation, Water Sci. Technol. 55 (2007) 145–153.

[15] C. Allegre, P. Moulin, M. Maisseu, F. Charbit, Treatment and reuse of reactive dyeing effluents, J. Membr. Sci. 269 (2006) 15–34.

[16] N. Kulik, Y. Panova, M. Trapido, The fenton chemistry and its combination with coagulation for treatment of dye solutions, Sep. Sci. Technol. 42 (2007) 1521–1534.

[17] E. Guibal, J. Roussy, Coagulation and flocculation of dye-containing solutions using a biopolymer (chitosan), React. Funct. Polym. 67 (2007) 33–42.

[18] J.S. Wu, C.H. Liu, K.H. Chu, S.Y. Suen, Removal of cationic dye methyl violet 2B from water by cation exchange membranes, J. Membr. Sci. 309 (2008) 239–245.

[19] S. Karaca, A. Gurses, M. Acıkyıldız, M. Ejder, Adsorption of cationic dye from aqueous solutions by activated carbon, Micropor. Mesopor. Mater. 115 (2008) 376–382.

[20] S.S. Tahir, N. Rauf, Removal of a cationic dye from aqueous solutions by adsorption onto bentonite clay, Chemosphere 63 (2006) 1842–1848.

[21] C.H. Weng, Y.F. Pan, Adsorption of a cationic dye (methylene blue) onto spent activated clay, J. Hazard. Mater. 144 (2007) 355–362.

[22] K.S. Alpat, O. Ozbayrak, S. Alpat, H. Akcay, The adsorption kinetics and removal of cationic dye, toluidine blue O, from aqueous solution with Turkish zeolite, J. Hazard. Mater. 151 (2008) 213–220.

[23] B. Noroozi, G.A. Sorial, H. Bahrami, M. Arami, Equilibrium and kinetic adsorption study of a cationic dye by a natural adsorbent-silkworm pupa, J. Hazard. Mater. B 139 (2007) 167–174.

[24] W.T. Tsai, H.C. Hsub, T.Y. Su, K.Y. Lin, C.M. Lin, T.H. Dai, The adsorption of cationic dye from aqueous solution onto acid-activated andesite, J. Hazard. Mater. 147 (2007) 1056–1062.

[25] R.F. Ziolo, E.P. Giannelis, B.A. Weinstein, M.P. Ohoro, B.N. Ganguly, V. Mehrotra, M.W. Russell, D.R. Huffman, Matrix-mediated synthesis of nanocrystalline γ-Fe_2O_3. A new optically transparent magnetic material, Science 257 (1992) 219–223.

[26] J. Ge, Q. Zhang, T. Zhang, Y. Yin, Core–satellite nanocomposite catalysts protected by a porous silica shell: controllable reactivity, high stability, and magnetic recyclability, Angew. Chem. Int. Ed. 47 (2008) 8924–8928.

[27] M. Shokouhimehr, Y. Piao, J. Kim, Y. Jang, T. Hyeon, A magnetically recyclable nano-composite catalyst for olefin epoxidation, Angew. Chem. Int. Ed. 46 (2007) 7039–7043.

[28] Q.Q. Liu, L. Wang, A.G. Xiao, H.J. Yu, Q.H. Tan, J.H. Ding, G.Q. Ren, Unexpected behavior of 1-chlorodecane as a novel porogen in the preparation of high-porosity polydivinyl-benzene microspheres, J. Phys. Chem. C 112 (2008) 13171–13174.

[29] Q.Q. Liu, L. Wang, A.G. Xiao, H.J. Yu, Q.H. Tan, A hyper-cross-linked polystyrene with nano-pore structure, Eur. Polym. J. 44 (2008) 2516–2522.

[30] Z. Zhang, E. Chalkova, M. Fedkin, C. Wang, S.N. Lvov, S. Komarneni, T.C.M. Chung, Synthesis and characterization of poly(vinyldene fluoride)-g-sulfonated polystyrene graft copolymers for proton exchange membrane, Macromolecules 41 (2008) 9130–9139.

[31] F.M. Winnik, A. Morneau, R.F. Ziolo, H.D.H. Stover, W.H. Li, Template-controlled synthesis of superparamagnetic goethite within macroporous polymer microspheres, Langmuir 11 (1995) 3660–3666.

[32] J. Zhang, S. Xu, E. Kumacheva, Reactors for semiconductor, metal, and magnetic nanoparticles, J. Am. Chem. Soc. 126 (2004) 7908–7914.

[33] V.K. Gupta, A. Mittal, V. Gajbe, J. Mittal, Adsorption of basic fuchsin using waste materials-bottom ash and deoiled soya-as adsorbents, J. Colloid Interface Sci. 319 (2008) 30–39.
[34] A. Mittal, V. Gajbe, J. Mittal, Removal and recovery of hazardous triphenylmethane dye, methyl violet through adsorption over granulated waste materials, J. Hazard. Mater. 150 (2008) 364–375.
[35] B. Bhole, B. Ganguly, A. Madhuram, D. Deshpande, J. Joshi, Biosorption of methyl violet, basic fuchsin and their mixture using dead fungal biomass, Curr. Sci. 86 (2004) 1641–1645.
[36] D. Solpan, Z. Kölge, Adsorption of methyl violet in aqueous solutions by poly(N-vinyl-pyrrolidone-co-methacrylic acid) hydrogels, Radiat. Phys. Chem. 75 (2006) 120–128.
[37] D. Solpan, S. Durana, D. Saraydinb, O. Guven, Adsorption of methyl violet in aqueous solutions by poly(acrylamide-co-acrylic acid) hydrogels, Radiat. Phys. Chem. 66 (2003) 117–127.
[38] M. Dogan, M. Alkan, Removal of methyl violet from aqueous solution by perlite, J. Colloid Interface Sci. 267 (2003) 32–41.